# Location and Fault Detection of Catenary Support Components Based on Deep Learning

Zhigang Liu, *Senior Member,* Junping Zhong, Yang Lyu, Kai Liu, Ye Han, Liyou Wang, Wenqiang Liu

***Abstract*—Catenary support components (CSCs) are the most important devices that support the overhead line and messenger of catenary system in electric railway. The faults of CSCs can result in the poor state of catenary system, and directly influence the normal operation of trains. In order to efficiently locate and identify the faults of CSCs, the deep learning algorithms are tried to process the captured images of CSCs in this paper. First at all, a dataset of CSCs that contains 50k labeled instances with 12 categories is built. Second, some traditional location methods of CSCs are introduced, and four recent representative deep learning networks, namely Faster RCNN (VGG16 and ResNet101), YOLOv2 and SSD, are applied to locate 12 categories CSCs, simultaneously and separately. In order to find more suitable algorithms of deep learning, their location performances are compared and evaluated. For the location of single category of CSCs, these algorithms show good performance. However, the models that are adopted to simultaneously locate all categories have a poor location performance on small-scale components of CSCs. Third, aiming at the fault detection of CSCs, some common methods are presented and compared, and the deep learning algorithms are tried to detect the faults of CSCs. Finally, the issues of deep learning for location and fault detection of CSCs, especially for the simultaneous location of CSCs are proposed and discussed, and further prospects are given.**

***Index Terms*—railway, catenary support components, deep learning, target location, faults detection**

## I. Introduction

CATENARY is an important part of the traction power supply system in high-speed railways, and it consists of some catenary support components (CSCs), such as Insulator, Rotary double ear, Brace sleeve. Fig. 1 shows the positions of all the crucial CSCs in the catenary system. The normal state of CSCs is the basis of the normal operation of high-speed trains. However, fault states of CSCs could occur due to the vibration caused by vehicles and the complex natural environment near the railway. Typical CSCs faults include breakage and fracture of the component, missing and looseness of the fasteners, and other fault states, as shown in Fig. 2. To ensure the power transmission from the catenary system to vehicles normally, it is essential to inspect the working states of CSCs. In this work, vision-based methods are generally used for CSCs inspection. The high-resolution cameras and LED lights are mounted on the top of a specific inspection vehicle, which moves along the railway and captures images of CSCs. Then intelligent algorithms are applied to process these images and detect the faults. Usually, the inspection of CSCs faults can be divided into two steps. First, CSCs are located in the raw image. Second, different fault detection methods are applied to different types of CSCs. At present, approaches are mainly based on the grayscale and edge information of located CSCs. If the location of CSCs is not accurate, the fault detection result may not be correct either. In the past decade, local feature descriptors such as SIFT (Scale-invariant feature transform) [1] descriptors, HOG (Histogram of Orientated Gradients) [2] features, LBP (Local Binary Pattern) [3] features and DPM (deformable part models) [4], have been popular and important methods in object location area. Although these methods can be used to locate CSCs, the accuracy needs to be improved when the image is complex. Besides, their processing speed is not fast enough for large amounts of captured images.

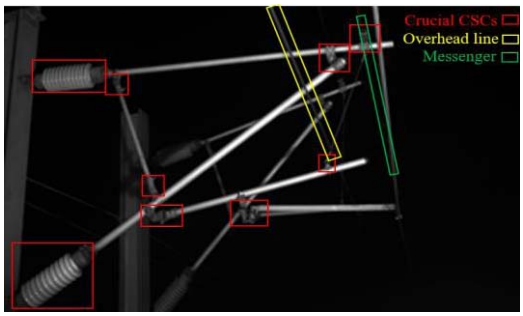


Fig. 1 Positions of CSCs in the catenary system

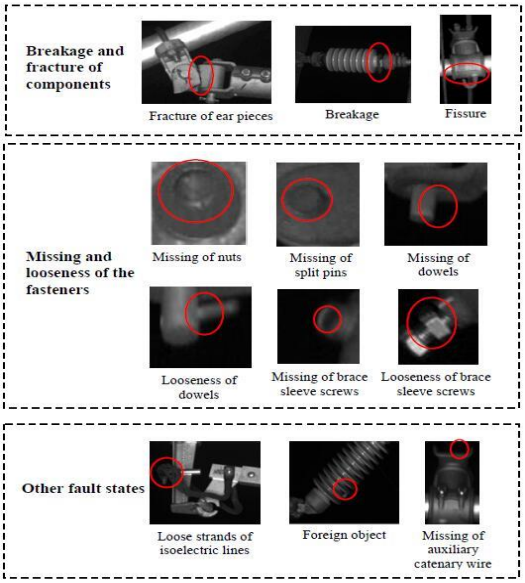


Fig. 2 Typical faults of different CSCs

Recently, deep learning has been developing fast and has achieved impressive improvements in several benchmark vision competition datasets, such as PASCAL VOC (pattern analysis, statistical modelling and computational learning, visual object classes) [5]. The networks used in object location can be divided into two types. The first type includes Fast RCNN (fast region-based convolutional networks) [6], Faster

978-1-5386-2222-3/18/$31.00 ©2018 IEEE

RCNN (Towards real-time object detection with region proposal networks) [7], and R-FCN (Region-based fully convolutional network) [8]. This type of networks is based on region proposals. Every region proposal in the image will be inputted to a sub-network for classification. The second type of networks includes YOLO (You only look once) [9] and SSD (Single shot multi-box detector) [10]. This type of networks is based on regression. Usually, regression based networks run faster than region proposal based networks does. For image classification task, the ResNet101 (101 layers residual network) [11] and VGG16 (Simonyan and Zisserman) [12] are the state-of-the-art classification deep networks. At present, deep learning has already been tried in railroad track inspection and rail plug detection [13-14], and impressive results have been achieved. It is likely to apply deep learning algorithms to CSCs location and faults detection effectively. The framework of this paper is shown in Fig. 3.

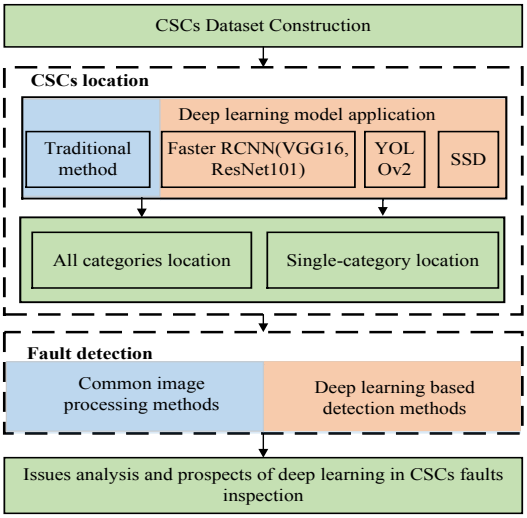


Fig. 3 The main frame of this paper

## II. LOCATION OF CSCS

### A. Construction of dataset

Dataset is very important in the field of deep learning for object location tasks. It provides large amounts of labeled targets for training and evaluating the proposed models. In recent years, some famous large-scale datasets such as PASCAL VOC [5], ImageNet [15] and Microsoft COCO [16] are built, and used for benchmark vision competitions. These datasets consist of a variety of categories, and the objects of each category have different scales and shapes. For example, the ImageNet contains 1000 categories, and each category has 500-1000 images. Category such as cat has different poses and sizes. In catenary system, the category number of CSCs is much smaller, and the CSCs usually do not change in shapes except for scale changing. Thus, the states of CSCs are less complex than objects in benchmark datasets. We can build a specific dataset for catenary system.

Table 1. The instance amounts of each category in catenary dataset

| Category | Amount | Category | Amount |
|---|---|---|---|
| Insulator | 4054 | Double sleeve connector | 3076 |
| Rotary double ear | 2749 | Messenger wire base | 3222 |
| Binaural sleeve | 2751 | Windproof wire ring | 2031 |
| Brace sleeve | 5211 | Insulator base | 4079 |
| Bracing wire hook | 2848 | Brace sleeve screw | 5328 |
| Steady arm base | 2917 | Isoelectric line | 1533 |

To build the dataset, 12 categories (see Fig. 4) of CSCs are chosen to annotate manually, and these CSCs are crucial to the catenary system and have a relative high risk to be in fault states. About 40000 instances in 6000 images are labeled, and each category instances have varieties of scales and poses. The instance amount of each category is shown in Tab. 1. In each category, half of the amount instances are randomly selected as the training samples and the rest as the testing samples. The deep learning models that implemented in this paper are all trained and tested in our built dataset.

### B. CSCs location based on traditional methods

The traditional approaches for CSCs location are mainly based on artificial features. They can be divided into three series. In the first series, grayscale values or straight-line characteristic are utilized directly, such as template matching based on cross correlation. For one category CSCs location, a variety of templates need to be selected to match the rectangular area of raw images. This method should manually choose the size of templates and rectangular areas, such as the work in [17]. In the second series, local invariant features are utilized for location, such as SIFT and SURF (speeded-up robust features). In [18-19], the location of Rotary double ears is realized by matching SIFT feature points between the raw image and the standard CSCs image. These methods are much robust than cross correlation calculation method, as local invariant features are less sensitive to scale and illumination change. However, the incorrect matches can still occur even in same simple cases, as shown in Fig. 5(a). In the third series, machine learning is applied to realize the classification and location. As shown in Fig. 5(b) left, a slide window is applied to the raw image and produce large amounts of candidate boxes. Then HOG features are extracted from each candidate box, a linear classifier, such as SVM (support vector machine), is trained based on the HOG features is applied to classify the candidate boxes. As the work in [20], AdaBoost algorithm is used to train cascade SVM classifiers that based on HOG feature to locate the Brace sleeve component, and some incorrect location can still occur, as shown in Fig. 5(b) right. In general, the traditional location approaches are less accurate and time-consuming, and they usually only location one category CSCs at one time.

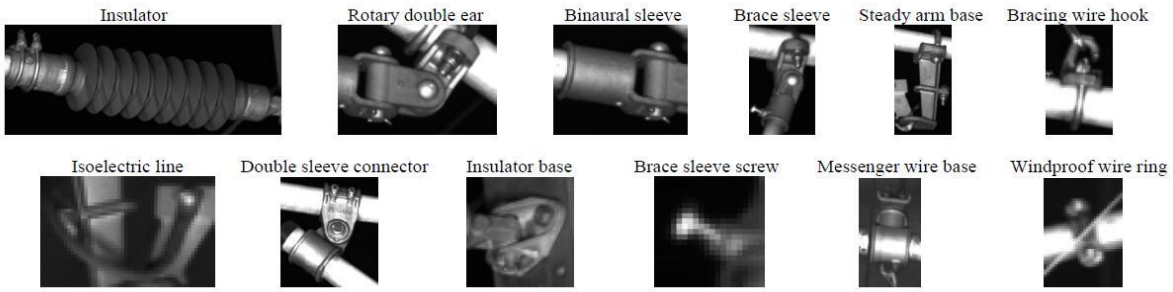


Fig. 4 12 categories of CSCs annotated in our dataset

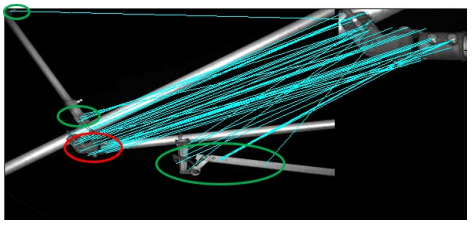


(a) Incorrect Rotary double ears location based on SIFT matching

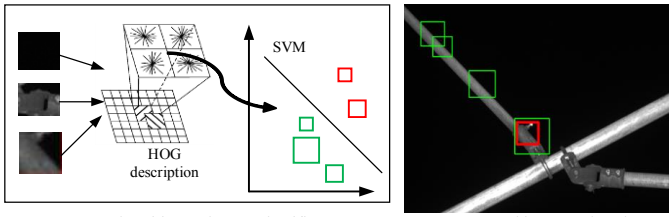


**Left:** HOG descrition and SVM classifier. **Right:** correct and incorrect location

(b) Brace sleeve location based on HOG and SVM

Fig. 5 Location approaches tried on some CSCs

### *C. CSCs location based on deep learning*

(1) Deep learning model for all categories location

According to the recent research, Faster RCNN [7], YOLOv2 [9] and SSD [10] are the representative deep learning models and are frequently used in comparisons to new methods. Thus, four models (VGG16 [12] and ResNet101 [11] are chosen as feature extractor of Faster RCNN, respectively) are trained and tested in the built dataset, and the location performance in catenary system is evaluated. All models are implemented in the deep learning framework Caffe [21] with the same training parameters as follows. Learning rate is set to 0.001 at the initial 3k iterations, and then is multiplied 0.1 between 3k and 8k iterations; finally the learning rate stays at 0.00005 between 8k and 15k iterations. The weight decay and momentum are set to be 0.0005 and 0.9, respectively. Non-maximum suppression (NMS) is applied to merge the initially detected bounding boxes with a threshold of 0.3 IoU (Intersection over Union). Other specifications and parameters follow the original configurations, respectively. The trained models are obtained after 15k iterations, and the loss functions have not decreased anymore.

Some located CSCs examples generated by the implemented deep learning models are shown in Fig. 6. In the testing, there are two indexes to evaluate location performance of each model, namely mAP (mean Average Precision) and FPS (frames per second). The mAP and FPS of four representative models are summarized in Tab. 2, which shows that all mAPs are in the range 0.52-0.80. Faster RCNN ResNet101 has the highest mAP 0.7972 and YOLOv2 has the highest FPS 3.70. For catenary system, mAP or AP (Average Precision) is considered as the primarily indexes because the detection accuracy is the most important.

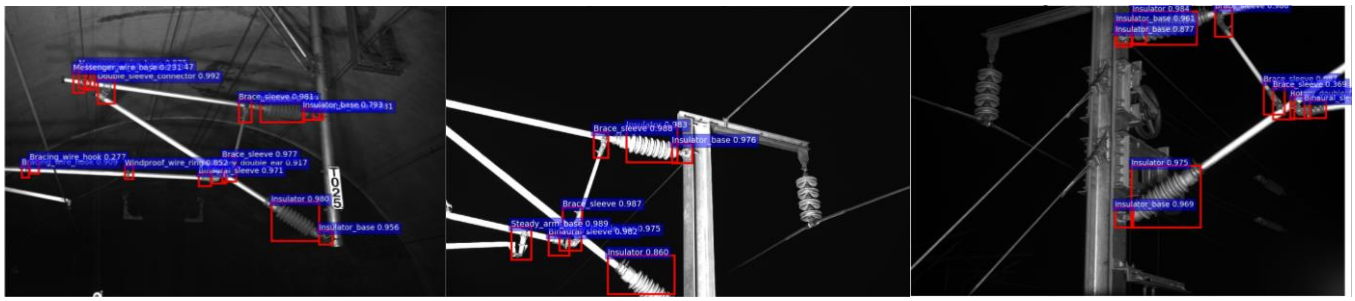

Fig. 6 Simultaneous CSCs location examples that generated by the implemented deep learning models. Each image is randomly selected

Table 2. Comparisons of mAP and FPS for four representative models

| Model | mAP | FPS |
|---|---|---|
| Faster RCNN ResNet101 | **0.797** | 1.97 |
| Faster RCNN VGG16 | 0.627 | 1.46 |
| SSD | 0.662 | 2.30 |
| YOLOv2 | 0.521 | **3.70** |

The columnar statistical figure of per-category AP for four models is shown in Fig. 7. It indicates that Faster RCNN ResNet101 performs best in all categories. SSD and Faster RCNN VGG16 perform the same performance in most of categories, and YOLOv2 performs well for locating large-scale components but poor for small-scale components. It clearly shows that detection performances on small targets, such as Brace sleeve screw, Windproof wire ring and Bracing wire hook, are far from satisfactory. The APs of SSD and Faster RCNN VGG16 for Brace sleeve screw are even zeros, and this issue cannot be ignored in the CSCs location.

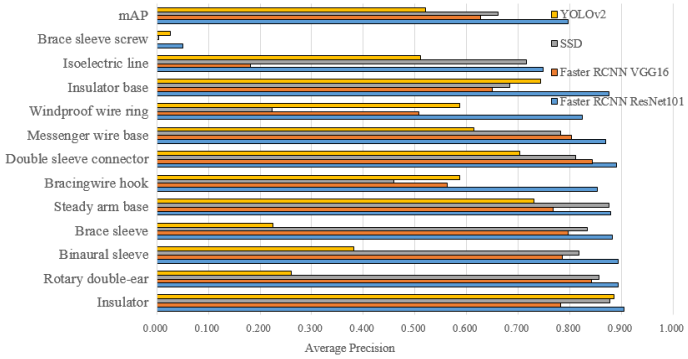


Fig. 7 Per-category AP comparison of the four models for location

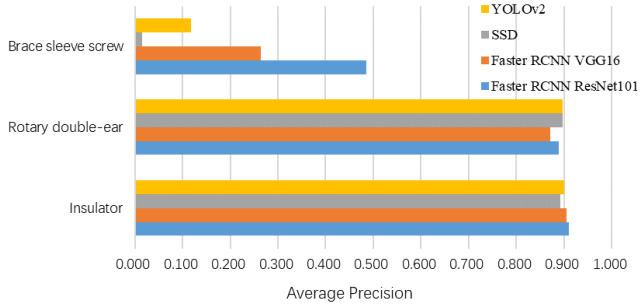


Fig. 8 APs of 12 representative models for a specified category

In this section, four deep learning models are applied to detect 12 categories CSCs at the same time. The test results show that Faster RCNN ResNet101 performs best in location accuracy on this dataset. All four representative models cannot completely adapt the catenary environment. They do not well enough on small CSCs, especially on Brace sleeve screw.

(2) Deep learning model for one category location

For a specific category, YOLOv2, SSD and Faster RCNN (VGG16, ResNet101) are adopted in this section. Three categories, namely Insulator, Rotary double ear and Brace sleeve screw, are chosen as they represent different sizes of CSCs. Thus, there are 12 models (four deep learning methods for three categories) to be trained. The training and testing parameters and specifications are similar to that in last section. One-category CSCs location examples are shown in Fig. 9. The statistical results of AP are summarized in Fig. 8 and Tab. 3. Compared with the Fig. 7, it shows that the performance of four methods are improved to some extent when detect three categories, and all models achieve high detection accuracy for the large and middle scale CSCs. The AP improvements of Faster RCNN VGG16 and Faster RCNN ResNet101 are obvious for small-scale targets. However, SSD and YOLOv2 still perform really badly.

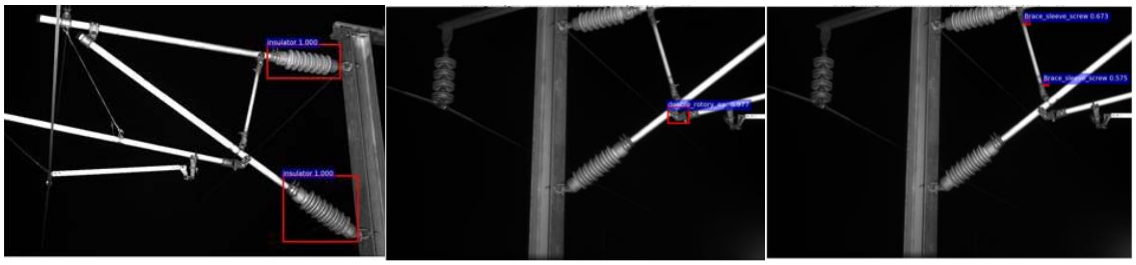

Fig. 9 Examples of one-category CSCs location and each image is randomly selected.

Table 3. mAP of 4 representative models with specified categories

| Model | Average Precision | | |
|---|---|---|---|
| | Insulator | Rotary double ear | Brace sleeve screw |
| Faster RCNN ResNet101 | 0.911 | 0.890 | 0.485 |
| Faster RCNN VGG16 | 0.905 | 0.872 | 0.264 |
| SSD | 0.893 | 0.897 | 0.015 |
| YOLOv2 | 0.901 | 0.898 | 0.118 |

Experiments in the *C* parts indicate that the one-category models can get better AP than multi-categories models based on the same deep learning network, especially for the location of small-scale targets.

### *D. Comparison of traditional and deep learning methods*

The traditional location of CSCs is mainly based on artificial features, which are less discriminative and robust. Incorrect matching and location may even occur in some simple cases. Besides, only one category of CSCs is usually located at a time and has time-consuming. It is obvious that traditional methods have low accuracy and lack of intelligence.

For the location based on deep learning methods, a combination of convolution layer, pooling layer and motivation layer can obtain high-level abstract and discriminative features, which can achieve the accurate location for most of CSCs. The experiments above have shown the deep learning methods are greatly superior to existing traditional methods in accuracy. Deep learning methods may even realize the real-time simultaneous location for all categories in some situations.

## III. FAULTS DETECTION

Our CSCs fault diagnosis system is a turnkey system. The previous location stage enables the application of faults detection.

### *A. The common image processing methods*

As different CSCs have different fault characteristics, some different faults detection methods can be proposed for the corresponding fault characteristic of CSCs. Some common methods [22, 19, 23, 20, 24] based on image processing have been tried for several important CSCs, such as Insulator, Rotary double ear, Brace sleeve screw, Isoelectric line and Messenger wire base. For the breakage and fracture faults detection of CSCs, the gradient and transformation information are usually utilized. In Fig. 10(a), the curvelet transform is applied to the located Insulator, and the abnormal region can be found by analyzing the curvelet coefficients, then the broken discs of Insulator is identified. In Fig. 10(b), the fracture of Rotary double ear can be detected by extracting the abnormal change

in gradient curve. Fig. 10(c) shows the crack detection on Messenger wire base by using Beamlet transform, which extracts the crack feature by the local curve search algorithm.

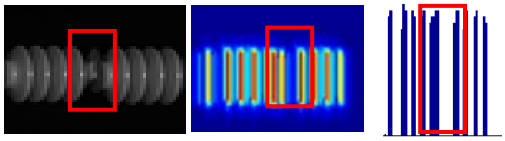

(a) curvelet transform for broken discs of Insulator detection

(b) fracture of Rotary double ear detection based on gradient

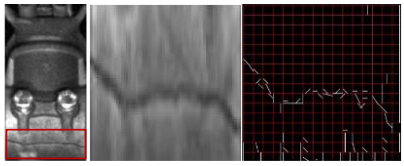

(c) Beamlet transform for crack of Messenger wire base detection

Fig. 10 Breakage and fracture faults detection on CSCs

The grayscale statistics and texture characteristics are also often used. In [20], grayscale values accumulation is utilized. As shown in Fig. 11, grayscale values accumulation is implemented on the located images of loose and normal states of Brace sleeve screw, respectively, in the specific direction. The values in the red circles are the discrimination information for fault detection. In [24], the isoelectric line is extracted by the iteration condition model/maximization of the posterior, marginal. The loose strands fault can be detected by the grayscale statistics in Fig. 12. The common detection methods firstly extract the grayscale, gradient or texture features of CSCs, and then the criteria need to be proposed manually and to identify the CSCs' states. The common methods can work well for some cases, but are not robust to complex conditions.

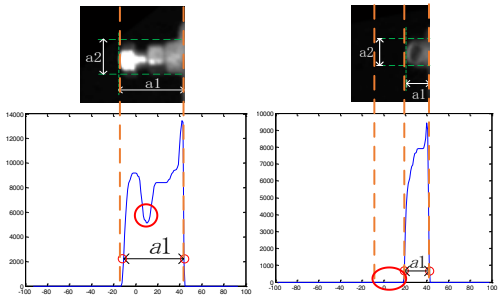


Fig. 11 Missing of Brace sleeve screw detection

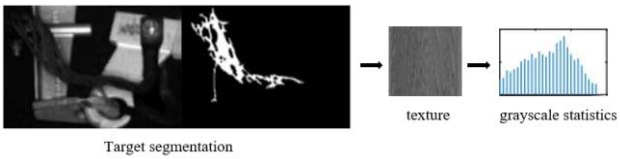


Fig. 12 Loose strands of Isoelectric line detection

## B. Deep learning methods

A direct application of supervised deep classification neural network may be a good method to detect all faults of different CSCs at the same time. In [25], we have tried to simultaneous detect the missing and looseness of fasteners, which including Split pins, Puller bolts, Screws and Nuts, by applying a deep convolutional neural network (DCNN). The architecture of the DCNN for classification is shown in Fig. 13.

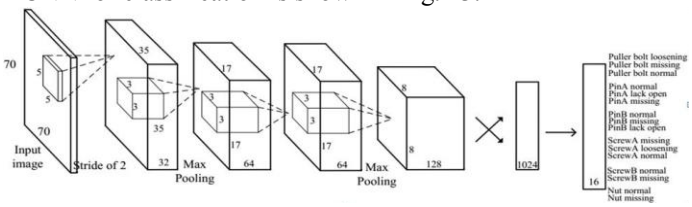


Fig. 13 Deep convolutional neural network for faults detection

This deep convolutional neural network contains four convolutional layers and two fully connected layers. The located sub-image is forwarded through the convolutional layers or pooling layer, and produces discriminative features. The output layer is connected to a 16-way softmax that produces the probabilities for 16-categories fastener states.

Compared with common image processing methods, deep learning methods do not need to give the fixed criteria or rules for faults states judgement, and their features are discriminative. In addition, their detection speeds are fast. However, unlike the missing and looseness of fasteners in [25], some other types of faults, such as the breakage of insulators and the ear pieces of rotary double ears, cannot be detected by the direct application of supervised deep learning network, because the numbers of these fault samples are limited, and robust classifiers cannot be trained as the over fitting would occur during training. We will give some prospects and advice for this issue in Section V.

# IV. Comparison and Further Prospects

For the fault detection of CSCs, compared with the traditional location and faults detection methods, although the deep learning method has achieved better results, there are still some issues that need to further research.

## A. Location issue of small targets

Four representative deep learning methods achieve poor results in the location of small-scale targets (i.e. Brace sleeve screw, whose pixel area accounts for about $2\times10^{-4}$ of the whole catenary image pixel area). Some reasons may lead to the location failure of small targets.

(r1) Feature loss of small-scale targets

To shorten the training time and reduce memory occupancy rate, the images used for training are shrunk and then are passed through the pooling layer of neural network. The discriminative feature of Brace sleeve screw may be lost. Besides, if the feature learned by network is too worse to describe the brace sleeve screw, it will result in poor location results.

(r2) The issue of region candidate box

For the methods of RCNN series, the anchors that sent to ROI (Region of Interest) pooling layer is sorted by softmax scores and these anchors scales are usually set manually, e.g. [128, 256, 512]. As there are few anchors that only contain a small target, these anchors may not be sent to ROI pooling layer and further be classified and regressed.

Since the structure of catenary system is relative fixed, and solving the small objects location problem can be considered.

(s1) Feature extraction network. For r1, to increase the size of the input image within a reasonable range during training

may help to solve this problem. However, this measurement will increase memory usage and training time. Reducing the number of pooling is an alternative solution. Large network is becoming more and more effective for the multi classification of images in complex scenes. Catenary images are relatively simple and do not need too many classifications. Maybe, designing a neural network with suitable depth and less pool layers will be a good solution.

(s2) Regression. For r2, it is known to all that the brace sleeve screw exists as the part of brace sleeve. Using this characteristic, the position of the brace sleeve can be preliminary obtained by a simple neural network. During the training, the preliminary obtained position can be sent to ROI pooling layer by force. Therefore, the position information of brace sleeve screw can be integrated into the high-layer feature maps. In addition, changing the scales of anchors is also an alternative solution.

### *B. The improvement of AP (Average Precision)*

According to experimental results, the largest value of AP is around 0.9. Accuracy of 0.9 is a good result, but it is promising to further improve the location accuracy. Increasing the number of iterations may increase the AP value to some extent. How to improve the AP of each category needs to be further studied.

### *C. Fault detection*

For CSCs, the fault samples are limited. The fault detection process is carried out alone after CSCs location, and the fault detection is still processed by common methods. For small amounts of fault samples, how to integrate the fault detection process into deep neural network needs to be studied. Several measurements to increase the fault samples can be considered.

(1) According to the railway personnel experience, 3D modelers can simulate the surface texture and shape of faulty components in a real environment. The generated images in a virtual environment are used as the training samples and the combination of transfer learning may produce good effects.

(2) Producing fault samples using generative adversarial networks (GAN) [26] may be a research direction that can be attempted.

## V. CONCLUSION

This paper presents the work that we have tried for CSCs location and faults detection, especially the work of deep learning. The experiment results indicate that deep learning methods can realize CSCs location with high accuracy for most categories, and they are also promising for faults classification. Finally, our views on some issues in the CSCs location and fault detection are given, and several potential solutions are proposed to help solving the problems in this field.

## REFERENCES


[1] D. G. Lowe, "Distinctive image features from scale-invariant key points," *International Journal of Computer Vision*, vol. 60, no. 2, pp. 91-110, 2004.

[2] N. Dalal, and B. Triggs, "Histograms of oriented gradients for human detection," *IEEE Conference on Computer Vision and Pattern Recognition*, San Diego, pp. 886-893, June. 20-25, 2005.

[3] X. Wang, T. X. Han, and S. Yan. "An hog-lbp human detector with partial occlusion handling," *IEEE International Conference on Computer Vision*, Tyoto, pp. 32-39, Sep. 29-Oct. 02, 2009.

[4] P. F. Felzenszwalb, R. B. Girshick, D. Mcallester, and D. Ramanan, "Object detection with discriminatively trained part-based models," *IEEE Transactions on Pattern Analysis and Machine Intelligence*, vol. 32, no. 9, pp. 1627-1645, 2010.

[5] M. Everingham, L. Gool, C. Williams, J. Winn, et al., "The pascal visual object classes (VOC) challenge," *International Journal of Computer Vision*, vol. 88, no. 2, pp. 303-338, Jun. 2010.

[6] R. B. Girshick, "Fast R-CNN," *IEEE Conference on Computer Vision and Pattern Recognition*, Santiago, pp. 1440-1448, Dec. 11-18, 2015.

[7] S. Ren, K. He, R. Girshick, and J. Sun, "Faster R-CNN: towards real-time object detection with region proposal networks," *IEEE Transactions on Pattern Analysis & Machine Intelligence*, vol. 39, no. 6, pp. 1137-1149, Jun. 2015.

[8] J. Dai, Y. Li, K. He, et al., "R-FCN: Object detection via region-based fully convolution networks," *arXiv preprint arXiv: 1605.06409,* 2016.

[9] J. Redmon, S. Divvala, R. Girshick, and A. Farhadi, "You only look once: unified, real-time object detection," in *IEEE Conference on Computer Vision and Pattern Recognition*, 2016, pp. 779-788.

[10] W. Liu, D. Anguelov, D. Erhan, C. Szegedy, S. Reed, C. Fu, and A. Berg, "SSD: Single Shot MultiBox Detector," in *European Conference on Computer Vision*, 2016, pp. 21-37.

[11] K. M. He, X. Y. Zhang, S. Q. Ren, et al., "Deep residual learning for image recognition," *IEEE International Conference on Computer Vision and Pattern Recognition*, Las Vegas, pp. 770-778, Jun. 26-Jul. 01, 2016.

[12] K. Simonyan, and A. Zisserman, "Very deep convolutional networks for large-scale image recognition," arXiv: 1409. 1556, 2014.

[13] X. Gibert, V. M. Patel, and R. Chellappa, "Deep multitask learning for railway track inspection," *IEEE Transactions on Intelligent Transportation Systems*, vol. 18, no. 1, pp. 153-164, 2017.

[14] F. Marino, A. Distante, P. L. Mazzeo, et al., "A real-time visual inspection system for railway maintenance: automatic hexagonal-headed bolts detection," *IEEE Transactions on Systems Man and Cybernetics Part C-Applications and Reviews*, vol. 37, no. 3, pp. 418-428, 2007.

[15] O. Russakovsky, J. Deng, H. Su, J. Krause, et al., "ImageNet large scale visual recognition challenge," *International Journal of Computer Vision*, vol. 115, no. 3, pp. 211-252, Sep. 2014.

[16] T. Lin, M. Maire, S. Belongie, J. Hays, et al., "Microsoft COCO: common objects in context," *arXiv preprint arXiv:1405.0312,* 2014.

[17] G. Zhang, Z. Liu, Y. Han, et al., "A fast fuzzy matching method of fault detection for rod insulators of high-speed railways," *Journal of the China Railway Society*, vol. 35, no.5, pp. 27-33, May. 2013.

[18] J. Zhong, Z. Liu, G. Zhang, et al., "Condition detection of swivel clevis pins in overhead contact system of high-speed railway," *Journal of the China Railway Society*, vol. 39, no. 6, pp. 65-71, Jun. 2017.

[19] H. Ye, Z. Liu, Z. Han, et al., "Fracture detection of ear pieces of catenary support devices of high-speed railway based on SIFT feature matching," *Journal of the China Railway Society*, vol. 36, no. 2, pp. 31-36, 2014.

[20] J. Chen, Z. Liu, Y. Han, et al. "Orientation and fault detection of diagonal tube in high-speed railway overhead contact system based on local feature description," *Journal of The China Railway Society*, vol. 39, no.11, 2017.

[21] Y. Q. Jia, E. Shelhamer, J. Donahue, et al., "Caffe: convolutional architecture for fast feature embedding," arXiv: 1408.5093, 2014.

[22] Z. Han, Z. Liu, H. Yang, and Y. Han, "Insulator fault detection based on curvelet coefficients morphology and zonal energy method," *Journal of the China Railway Society*, vol. 35, pp. 36-40, no. 3, Mar. 2013.

[23] K. Liu, Z. Liu, and J. Chen, "Crack detection of messenger wire supporter in catenary support devices of high-speed railway based on Faster R-CNN," *Journal of the China Railway Society*, 2017, accepted.

[24] Z. Liu, L. Wang, C. Li, et al., "A high-precision loose strands diagnosis approach for isoelectric line in high-speed railway," *IEEE Transactions on Industrial Informatics,* 10.1109/TII.2017.2774242.

[25] J. Chen, Z. Liu, H. Wang, et al., "Automatic defect detection of fasteners on the catenary support device using deep convolutional neural network," *IEEE Transactions on Instrumentation and Measurement*, 10.1109/TIM.2017.2775345.

[26] I. Goodfellow, J. Pouget-Abadie, M. Mirza, et al., "Generative adversarial nets," in *International Conference on Neural Information Processing Systems*, pp. 2672-2680, 2014.